

High quality electron beam generation in a proton-driven hollow plasma wakefield accelerator

Authors:

Yangmei Li^{1,2,*}, Guoxing Xia^{1,2,*}, Konstantin V. Lotov^{3,4}, Alexander P. Sosedkin^{3,4}, Kieran Hanahoe^{1,2}, Oznur Mete-Apsimon^{1,2,5}

Affiliations:

¹School of Physics and Astronomy, University of Manchester, Manchester M13 9PL, UK.

²Cockcroft Institute, Warrington WA4 4AD, UK.

³Budker Institute of Nuclear Physics, Novosibirsk 630090, Russia.

⁴Novosibirsk State University, Novosibirsk 630090, Russia.

⁵Department of Engineering, Lancaster University, Lancaster LA1 4YW, UK.

Correspondence and requests for materials should be addressed to G. X. Xia (guoxing.xia@manchester.ac.uk) or Y. M. Li (yangmei.li@postgrad.manchester.ac.uk).

Proton-driven plasma wakefield accelerators have numerically demonstrated substantially higher accelerating gradients compared to conventional accelerators and the viability of accelerating electrons to energy frontier in a single plasma stage. However, due to the intrinsic strong and radially varying transverse fields, the beam quality is still far from suitable for practical application in future colliders. Here we propose a new accelerating region which is free from both plasma electrons and ions in the proton-driven hollow plasma channel. The high quality electron beam is therefore generated with this scheme without transverse plasma fields. The results show that a 1 TeV proton driver can propagate and accelerate an electron beam to 0.62 TeV with correlated energy spread of 4.6% and well-preserved normalized emittance below 2.4 mm mrad in a single hollow plasma channel of 700 m. More importantly, the beam loading tolerance is significantly improved compared to the uniform plasma case. This high quality and high charge beam may pave the way for the development of future plasma-based energy frontier colliders.

Particle beam driven plasma-based accelerators (PWFA) have achieved enormous progress in recent decades^{1,2} and have experimentally demonstrated an energy record of 85 GeV in electron driven acceleration³. The achievable energy gain in a single stage is, however, limited by the transformer ratio⁴. Multi-stage acceleration was proposed to accelerate particles to the energy frontier (\sim TeV)^{5,6}. Nevertheless, in the near future PWFA-based accelerators with several tens of stages suitable for energy frontier collider applications will still be challenging technically⁷⁻¹¹.

Proton-driven plasma accelerators have numerically demonstrated electron acceleration up to TeV-level over a single hundreds of meters long uniform plasma channel¹²⁻¹⁴. However, unlike the electron driver, the positively charged driver attracts plasma electrons rather than fully expels them away and forms an electron-free bubble. This makes the transverse wakefield vary along the witness bunch and become radially nonlinear. The resultant radial force could significantly change the witness beam dynamics and degrade the beam quality in a long acceleration distance. Additionally, as plasma electrons oscillate with a larger spread in frequencies, the excited wakefield gradient is less than for the electron driven case under the same condition²³.

Hollow plasmas are free from the aforementioned issues¹⁵⁻²⁵. The hollow channel provides guiding for a laser or particle beam and forms an ion-free region with nearly zero or weak and linear transverse field, which benefits focusing and helps preserve a high quality of the witness bunch. Recently, an encouraging experiment at FACET of SLAC National Accelerator Laboratory has demonstrated an 8 cm long hollow plasma channel with a radius of 250 μm and the measured decelerating gradient on the driving positron beam reaches 230 MeV/m¹⁵. This opens up prospects for practical applications of hollow plasmas in plasma wakefield acceleration.

Earlier theoretical studies of hollow channels were mostly focused on low amplitude waves and linearly responding plasmas¹⁷⁻²⁴ and on laser¹⁷⁻²⁰ or electron²¹ drivers that push plasma electrons aside rather than pull them deeply into the channel. Studies of positively charged drivers are fewer in number²³⁻²⁷, but a good acceleration regime was found for this configuration²⁷. In this regime, a wide area void of both plasma electrons and ions exists in the channel, in which the accelerating field is as high as of the order of the wave-breaking limit. This regime opens path to accelerating a considerable amount of charge to TeV-range energies with low emittance and energy spread.

Yi et al.²⁷ have numerically demonstrated efficient acceleration of positrons in a strongly nonlinear wave driven by a short proton bunch in a hollow plasma channel. In their studies, the witness obtained not only high energy, but also preserved the normalized emittance and reached the final energy spread of 1.5%. However, future energy frontier colliders need both electrons and positrons with high energy and high quality. In this article, we propose and investigate electron acceleration driven by high energy proton bunches in a hollow plasma and demonstrate remarkable advantages of such an acceleration scheme. Our study differs in the way the results are obtained from ref. 27 because of nonlinear plasma behavior and its asymmetry with respect to the charge of witness beams. We locate the witness beam in the electron-free region that resembles the advantageous bubble structure in the uniform plasma driven by electrons except for the absence of ions. Because this region is completely free from transverse forces near the axis, such structure with high accelerating gradients but enormously reduced transverse wakefields is ideal for the witness beam²⁸. As a result, after stable acceleration over a long distance, almost all injected electrons reach over 60% of the driver energy while high beam quality is preserved. Furthermore, there is a possibility of simultaneously having high witness charge and high accelerating field, as

in the strong blowout regime²⁹, which enables high energy transfer efficiencies to be achieved.

Results

In the 2D particle-in-cell (PIC) simulations, a 150 μm long proton drive bunch with a typical energy of 1 TeV is adopted. This proton bunch is assumed to be compressed by a factor of around 1000 from the actual bunches produced in proton synchrotrons¹², such as the LHC or Tevatron. The bunch population is set as 1.15×10^{11} , which is the nominal value of the LHC. Quadrupoles are used to confine the head of the proton driver, but they also play a critical role in the transverse dynamics of the witness bunch. The witness electron bunch is assumed to have an initial energy of 10 GeV so that the external quadrupole fields focus both the drive and witness bunches well. The detailed explanation and also description of other parameters can be found in the Methods section. In our simulation a vacuum channel with a radius $r_c = 350 \mu\text{m}$ is introduced into the uniform plasma. The plasma ring ($r > r_c$) density is $5 \times 10^{14} \text{cm}^{-3}$. Ref. 25 demonstrates the feasibility of a hollow plasma, although there will be technological challenges to produce a single long plasma stage and further work needs to be done to realize the scheme in a single or multiple stages.

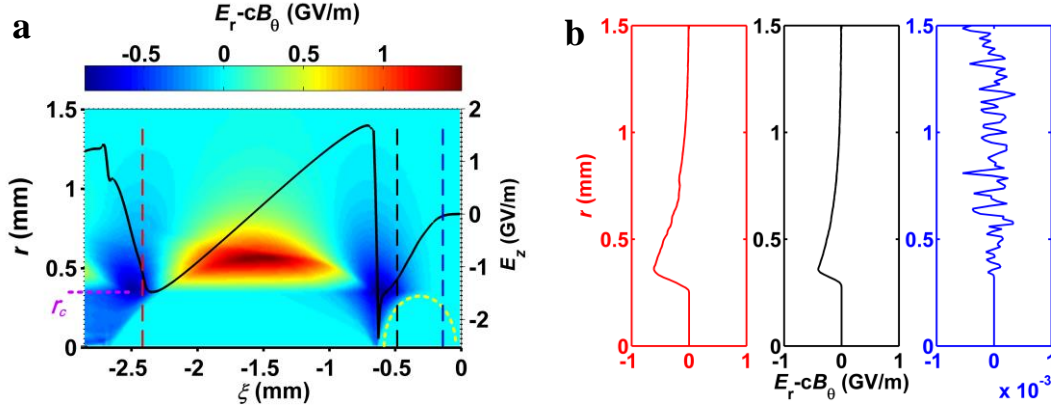


Figure 1 | Transverse and longitudinal fields at the beginning of interaction. (a) The on-axis longitudinal electric field is described by the black line. The yellow dashed curve and the purple dashed line illustrates the outline of the DB and the hollow boundary respectively. The red, black and blue vertical dashed lines mark the longitudinal midpoint of the WB, the rear and the front of the DB respectively. (b) The radial variations of the transverse fields at these three positions are illustrated with the corresponding colors. The simulation window travels to the right at the speed of light.

The initial transverse field distribution and the on-axis electric field are illustrated in Fig. 1. Note that the external magnetic fields from quadrupoles are not included into the transverse fields here. The witness bunch (WB) is initially placed slightly off the peak accelerating field of 1.4 GV/m. The transformer ratio is about 1 due to nearly equal peak accelerating field of the WB and the peak decelerating field of the drive bunch (DB). There are strong transverse fields at the regions where plasma electrons approach the axis, but as the WB and the DB are far from these regions, their dynamics is not affected. A larger wavelength of the wakefield compared to the wall plasma wavelength is beneficial to relax the requirement on synchronization of the WB. Fig. 1b shows that the transverse plasma wakefield acting on the WB is exactly zero, implying that the WB is free from transverse variation of the plasma wakefield. At the position marked by the black

dashed line in Fig. 1a, the radial field is also zero for protons located within the radius of 0.28 mm but strongly negative beyond that which will focus protons located at larger radii. As roughly seen from Fig. 1a, the zero radial fields cover the main part of the DB and there are strong focusing fields in larger radii at the rear part of the DB. Such a radial field structure is helpful in preserving the DB quality and thus extending the acceleration distance. The radial plasma fields at the front of the DB are insignificant, thus external quadrupoles are needed to ensure long distance propagation.

Fig. 2a shows that the witness electron bunch can be accelerated to 0.62 TeV with the relative energy spread of 4.6% after 700 m propagation in hollow plasma. The beam energy increases linearly within the initial 400 m, afterwards the increase of the bunch energy slows down. Still, the average accelerating gradient is over 1.0 GV/m before 590 m. The decreasing growth rate of bunch energy can be explained via the evolution of the on-axis longitudinal electric field illustrated in Fig. 2b. We see that the longitudinal wakefield pattern moves back with respect to the WB, but the average accelerating field experienced by the WB remains almost constant in the initial 400 m, then the maximum field gradually decreases and slips away from the WB. The phase slippage results from the relatively low relativistic factor of the DB. In order to alleviate this adverse effect, the WB is initially put at the left side of the maximum accelerating field (see Fig. 1a) to postpone the time when the WB slips out of the effectively accelerating region, but this is associated with the sacrifice of increasing the energy spread. Fortunately, the phase shift will eventually make the WB slip into an increasing accelerating field from the bunch front to the end, which helps minimize the energy spread. In order to compromise between energy gain and energy spread, the effective accelerating length is considered to be 700 m. Beyond that the WB can still extract energy from plasma waves but its energy spread shows an ascending trend. Moreover, the WB nearly slips out of the accelerating region and the accelerating gradient seen is essentially small. The energy increase is very inefficient in this case, thus the acceleration can be truncated after this length.

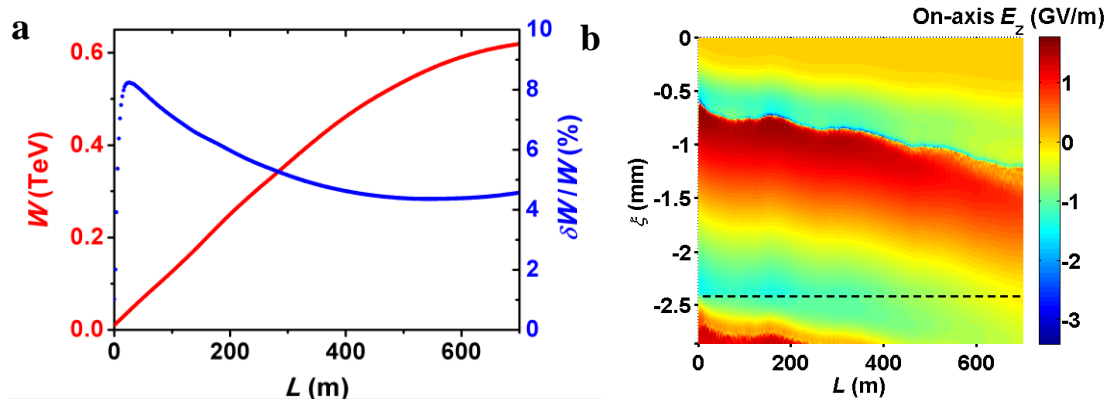


Figure 2 | Mean energy, energy spread and evolution of the on-axis longitudinal field. Evolution of mean witness beam energy and the relative energy spread (a) and the on-axis longitudinal electric field (b) with the acceleration distance. The black dashed line in (b) marks the longitudinal midpoint of the WB during the whole acceleration process.

Fig. 3a describes the evolution of the transverse field observed at the midplane of the WB. Electrons located at the other parts of the WB experience similar transverse field evolution, which

is therefore not given here. We see that in the initial 400 m the WB is located in a large region (in the hollow channel) completely without plasma wakefields, afterwards a negative transverse field starts acting on the outer region of the WB. This is because after 400 m propagation in plasma, the WB significantly slips towards the DB and goes into a region which is partially filled with plasma electrons attracted to the channel from the plasma wall. The negative fields could cause the divergence of witness electrons, leading to degradation of the beam emittance and loss of electrons. However, as the WB has a small initial beam radius which can be further reduced during acceleration and is additionally focused by the quadrupoles, the negative field region will not act on the WB. Fig. 4 shows that after the acceleration, almost all the witness electrons survive. The survival rate here is defined as the ratio of the number of electrons present in the final accelerated bunch to the number of initially injected electrons. Note that electrons considered here are located within 3 times initial beam radius, which is an effective beam width for applications. Furthermore, over 98% of protons survive, indicating that the external quadrupoles are appropriately set.

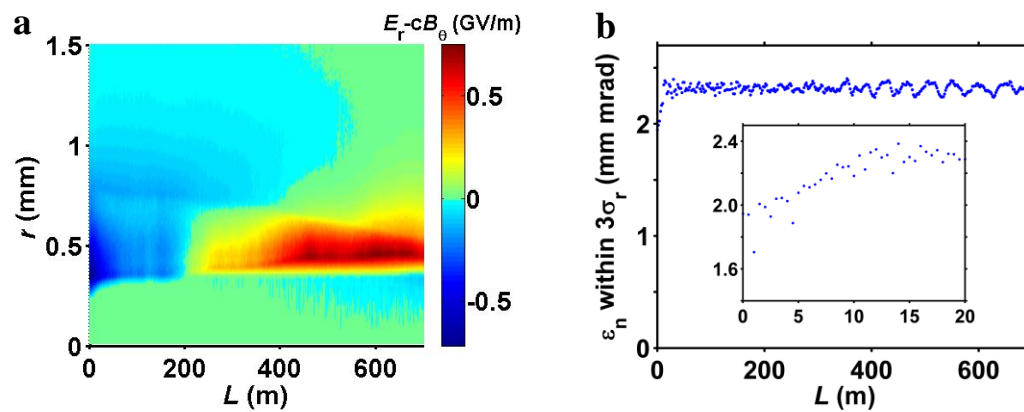


Figure 3 | Evolution of the transverse field and the normalized emittance. Evolution of radial variance of the transverse field observed along the middle of the WB (a) and the normalized emittance of witness electrons located within 3 times initial beam radius (b) with the acceleration distance. The inset in (b) illustrates the normalized emittance in the first 20 m.

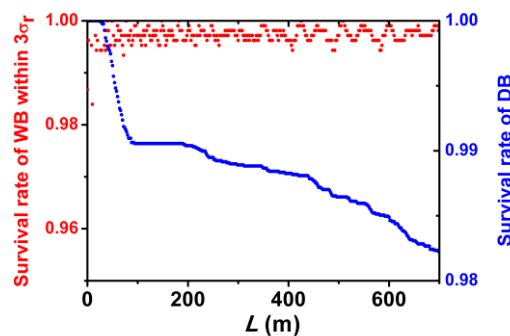


Figure 4 | Survival rates. Survival rates of witness electrons located within 3 times initial beam radius and the DB versus the acceleration distance.

As seen from Fig. 3b, the normalized emittance of the WB is conserved within a small value of 2.4 mm mrad. The inset of Fig. 3b indicates that a slight increase of beam emittance from the initial 1.95 mm mrad to 2.4 mm mrad occurs in the first 15 m. This is because the initial WB

radius (10 μm) is larger than the equilibrium one (7.6 μm) calculated based on ref. 13. Since there are no transverse plasma wakefields acting on the WB during the whole acceleration, the initial emittance growth comes from the external focusing of quadrupoles. More specifically, during acceleration the increasing beam energy spread causes frequency variation in betatron oscillations and phase mixing occurs. The incoherence of particle oscillations results in the emittance growth, but after 15 m when the beam matches with the focusing structure, the normalized emittance levels off.

Discussion

It is illustrated in Fig. 5 that for larger numbers of witness electrons the accelerating crest deforms to a flat top. However, this flat top does not coincide with the WB position. The WB actually experiences a decreasing gradient from the front to the back, which leads to growth in its energy spread. When loading 2.4 nC witness electrons, the corresponding on-axis accelerating field seen by the WB in the hollow plasma changes maximally from 1.38 GV/m to 1.11 GV/m. The variation extent is much less than for the uniform case in ref. 12 which is loaded with the same population of electrons. Note that here (and only here) the WB is initially put at a different position from Fig. 1a in order to clearly compare the field variations with ref. 12. A possible reason for mitigated beam loading effect in the hollow channel is that, there are no plasma electrons and ions in the vicinity of the WB, which makes the loading of substantial charges insignificant to the wakefield. The advantage seems more convincing considering the witness bunch length here is much shorter than that in ref. 12, i.e. its beam density is much higher.

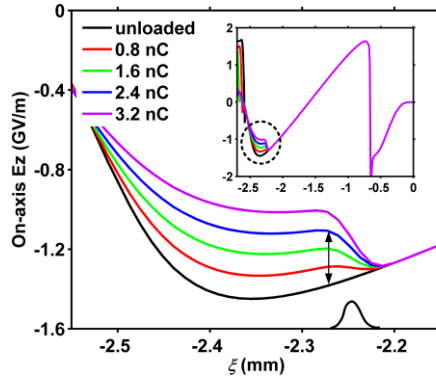


Figure 5 | On-axis accelerating fields. The on-axis accelerating fields for the unloaded and different particle population loaded cases in hollow plasma. The arrow marks the maximum change of the field seen by the WB from the unloaded to the 2.4 nC loaded case.

The final energies and the corresponding energy spread for various witness charges and other parameters unchanged are illustrated in Fig. 6. The simulation result shows that the final energy reduces with increasing beam charge, which results from lower accelerating fields seen by the WB due to a larger beam loading effect. As the accelerating gradient along the WB varies more steeply with the increasing bunch charge, the energy spread increases accordingly. Conversely, when loading fewer particles like 0.8 nC, the longitudinal wakefield seen by the WB is almost constant, thus the energy spread can be as low as 1.5% (see Fig. 6). Another approach to reduce the energy spread is to match the witness bunch length with the wave. In our case, the bunch is not matched

(shorter). Fig. 6 implies that after doubling the bunch length, its energy spread decreases from 4.6% to 2.1%. The decrease in mean energy is insignificant. The most attractive feature of the proposed hollow scheme is that the normalized emittance of the WB can still be preserved when accelerating a larger quantity of electrons. Fig. 7 shows that the normalized emittance remains below 2.5 mm mrad even when loading up to 3.2 nC of witness electrons. In principle, as long as the WB is located at the electron-free region formed in the hollow channel, its normalized emittance is conserved. Nevertheless, this is with the cost of increasing energy spread for accelerating larger number of electrons. A compromise between the energy gain and the energy spread is obtainable via extension of the bunch length or tailoring the bunch shape^{20-21,29-32}, which is worth further investigation.

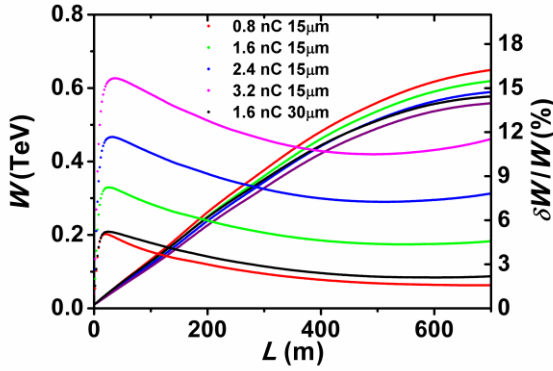


Figure 6 | Mean energy and energy spread for different loaded witness beams. Evolution of mean witness energies and the corresponding energy spread with the acceleration distance for different witness bunch beams.

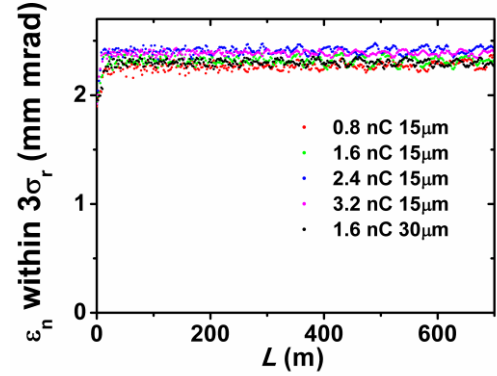


Figure 7 | Normalized emittance for different loaded witness beams. Evolution of normalized emittance with the acceleration distance for different witness beams.

In summary, we have discovered a good regime for plasma wakefield acceleration of electrons in hollow channels and illustrated it with simulations. The proposed scheme solves the issue of beam normalized emittance degradation due to radially varying and strong focusing forces in the uniform plasma driven by a positively charged drive beam. In this regime, the witness bunch is located in the region of both strong accelerating field and no plasma electrons inside. The region preserves its shape and location up to driver depletion, thus providing a high acceleration efficiency and the average transformer ratio of about unity. The witness beam takes advantage of hollow channels; it sees a radially uniform accelerating field and no transverse plasma fields. Therefore, the normalized beam emittance is conserved during acceleration, and the energy gain depends only on the longitudinal position along the bunch, thus enabling minimization of the energy spread by tailoring the bunch shape. The quadrupoles used to confine the driver from emittance-driven widening also play an important role in witness confinement. They keep the witness from entering the defocusing area that appears at large radii as the driver depletes.

Methods

The 2D PIC code LCODE^{33,34} using quasi-static approximation is employed to conduct hundreds of meters long simulations owing to its high computational efficiency. In the code, both the beam and the plasma are modeled by fully relativistic macro-particles. The simulation window using the

coordinate system (r, θ, ζ) travels with the speed of light c , where $\zeta = z - ct$. The window width is large enough to extend to the zero-field area so that the boundary condition is satisfied. The radial and axial grid sizes are set as $0.05c/\omega_p \approx 12 \mu\text{m}$. The time step is $8.404\omega_p^{-1} \approx 6.7 \text{ ps}$, corresponding to the length of 2 mm.

Beam and plasma parameters. Table 1 gives detailed parameters for beam, plasma and quadrupole magnets. The parameters are close to those in Ref.11, but slightly modified in search of the best acceleration regime. In particular, we reduce the beam radius to $350 \mu\text{m}$, increase the beam length to $150 \mu\text{m}$, and use the nominal population of LHC bunches to create the strongly nonlinear wake structure. The value of $r_c = 350 \mu\text{m}$ for the channel radius is chosen as a compromise between accelerating gradient and beam quality.

Table 1: Parameters for simulation

Parameters	Values	Units
Initial driving proton beam (DB):		
Proton population	1.15×10^{11}	
Initial energy	1	TeV
Energy spread	10%	
Longitudinal beam length	150	μm
Beam radius	350	μm
Angular spread	3×10^{-5}	
Initial witness electron beam (WB):		
Electron population	1.0×10^{10}	
Initial energy, W	10	GeV
Energy spread, $\delta W/W$	1%	
Longitudinal beam length	15	μm
Beam radius, σ_r	10	μm
Angular spread	1×10^{-5}	
Unperturbed hollow plasma:		
Plasma density, n_p	5×10^{14}	cm^{-3}
Hollow radius, r_c	350	μm
External quadrupole magnet:		
Magnetic field gradient, S	0.5	T/mm
Quadrupole period, L_q	0.9	m

Quadrupole parameters and the initial energy of the WB. The external quadrupoles were first proposed in ref. 7 to precisely align the trajectory of the driver and to prevent the emittance driven erosion of the driver head. For short proton drivers that propagate hundreds of meters, the quadrupole focusing becomes a must¹³. In hollow channels, not only the driver head but the whole driver and the witness are guided by quadrupoles, as there is no plasma focusing in the channel. According to ref. 13, the quadrupole focusing works properly (i.e., the radial oscillations of the particles are insignificant) when the focusing period of quadrupoles is much shorter than the period of transverse particle oscillations, that is,

$$L_q \ll 2\pi \sqrt{\frac{W}{eS}}. \quad (1)$$

Here L_q is the quadrupole period, W is the beam energy and S is the magnetic field gradient. For an achievable S of 0.5 T/mm and initial driver energy as W , the upper limit of L_q for the driver is 16 m. As the witness bunch has lower initial energy, the corresponding upper limit is smaller than for the driver. As the quadrupole magnets are built along the whole plasma channel, their period should satisfy the smaller upper limit, i.e. the one for the witness bunch. In addition, the simulation indicates that L_q should be larger than 0.9 m in order to guarantee that over 98% of protons survive after 700 m propagation in the hollow plasma. We choose $S = 0.5$ T/mm and $L_q = 0.9$ m as the optimal quadrupole parameters which requires a minimum quadrupole strength to sufficiently focus the driver. Based on the equation (1), the initial energy of the witness bunch must be much larger than 2.4 GeV. 10 GeV is chosen to keep radial oscillations of the witness bunch small. Eq. (1) also implies that the increase of the witness energy during the acceleration will gradually alleviate the limitation to the quadrupole period.

References

- [1] Litos, M. *et al.* High-efficiency acceleration of an electron beam in a plasma wakefield accelerator. *Nature* **515**, 92-95 (2014).
- [2] Corde, S. *et al.* Multi-gigaelectronvolt acceleration of positrons in a self-loaded plasma wakefield. *Nature* **524**, 442-445 (2015).
- [3] Blumenfeld, I. *et al.* Energy doubling of 42 GeV electrons in a metre-scale plasma wakefield accelerator. *Nature* **445**, 741-744 (2007).
- [4] Ruth, R. D., Chao, A. W., Morton, P. L. & Wilson, P. B. A plasma wake-field accelerator. *Part. Accel.* **17**, 171-189 (1985).
- [5] Cros, B. Plasma physics: Compact coupling for a two-stage accelerator. *Nature* **530**, 165-166 (2016).
- [6] Steinke, S. *et al.* Multistage coupling of independent laser-plasma accelerators. *Nature* **530**, 190-193 (2016).
- [7] Kudryavtsev, A. M., Lotov, K. V. & Skrinsky, A. N. Plasma wake-field acceleration of high energies: Physics and perspectives. *Nuclear Instr. Meth. A* **410**, 388-395 (1998).
- [8] Rosenzweig, J., Barov, N., Murokh, A., Colby, E. & Colestock, P. Towards a plasma wake-field acceleration-based linear collider. *Nuclear Instr. Meth. A* **410**, 532-543 (1998).
- [9] Adli, E. *et al.* Design of a TeV beam driven plasma wakefield linear collider. *Proc. IPAC13*, 1613 (2013).
- [10] Shiltsev, V. D. High energy particle colliders: past 20 years, next 20 years and beyond. *Physics - Uspekhi* **55**, 965 (2012).
- [11] Delahaye, J. P. *et al.* A beam driven plasma-wakefield linear collider from Higgs factory to multi-TeV. *Proc. IPAC14*, 3791 (2014).
- [12] Caldwell, A., Lotov, K. V., Pukhov, A. & Simon, F. Proton-driven plasma-wakefield acceleration. *Nature Phys.* **5**, 363-367 (2009).
- [13] Lotov, K. V. Simulation of proton driven plasma wakefield acceleration. *Phys. Rev. ST Accel. Beams* **13**, 041301 (2010).
- [14] Caldwell, A. & Lotov, K. V. Plasma wakefield acceleration with a modulated proton bunch. *Phys. Plasmas* **18**, 103301 (2011).

- [15] Gessner, S. *et al.* Demonstration of a positron beam-driven hollow channel plasma wakefield accelerator. *Nat. Commun.* **7**, 11785 (2016).
- [16] Marsh, K. A. *et al.* Positron beam propagation in a meter long plasma channel. *Proc. PAC-2003* (Oregon, USA), 731-733 (2003).
- [17] Chiou, T. C. *et al.* Laser wake - field acceleration and optical guiding in a hollow plasma channel. *Phys. Plasmas* **2**, 310-318 (1995).
- [18] Shvets, G., Wurtele, J. S., Chiou, T. C. & Katsouleas, T. C. Excitation of accelerating wakefields in inhomogeneous plasmas. *IEEE Trans. Plasma Sci.* **24**, 351 (1996).
- [19] Schroeder, C. B., Esarey, E., Benedetti, C. & Leemans, W. P. Control of focusing forces and emittances in plasma-based accelerators using near-hollow plasma channels. *Phys. Plasmas* **20**, 080701 (2013).
- [20] Schroeder, C. B., Benedetti, C., Esarey, E. & Leemans, W. P. Beam loading in a laser-plasma accelerator using a near-hollow plasma channel. *Phys. Plasmas* **20**, 123115 (2013).
- [21] Chiou, T. C. & Katsouleas, T. High beam quality and efficiency in plasma-based accelerators. *Phys. Rev. Lett.* **81**, 3411-3414 (1998).
- [22] Schroeder, C. B., Whittum, D. H. & Wurtele, J. S. Multimode analysis of the hollow plasma channel wakefield accelerator. *Phys. Rev. Lett.* **82**, 1177-1180 (1999).
- [23] Lee, S., Katsouleas, T., Hemker, R. G., Dodd, E. S. & Mori, W. B. Plasma-wakefield acceleration of a positron beam. *Phys. Rev. E* **64**, 045501 (2001).
- [24] Kimura, W. D., Milchberg, H. M., Muggli, P., Li, X. & Mori, W. B. Hollow plasma channel for positron plasma wakefield acceleration. *Phys. Rev. ST Accel. Beams* **14**, 041301 (2011).
- [25] Sahai, A. A. & Katsouleas, T. C. Optimal positron-beam excited plasma wakefields in hollow and ion-wake channels. *Proc. IPAC-2015* (Richmond, VA, USA), 2674-2677 (2015).
- [26] Yi, L. *et al.* Scheme for proton-driven plasma-wakefield acceleration of positively charged particles in a hollow plasma channel. *Phys. Rev. ST Accel. Beams* **16**, 071301 (2013).
- [27] Yi, L. *et al.* Positron acceleration in a hollow plasma channel up to TeV regime. *Sci. Rep.* **4**, 4071 (2014).
- [28] Assmann, R. & Yokoya, K. Transverse beam dynamics in plasma-based linacs. *Nucl. Instrum. Methods Phys. Res., Sect. A* **410**, 544-548 (1998).
- [29] Lotov, K. V. Efficient operating mode of the plasma wakefield accelerator. *Phys. Plasmas* **12**, 053105 (2005).
- [30] Katsouleas, T., Wilks, S., Chen, P., Dawson, J. M. & Su, J. J. Beam loading in plasma accelerators. *Part. Accel* **22**, 81-99 (1987).
- [31] Tzoufras, M. *et al.* Beam Loading in the Nonlinear Regime of Plasma-Based Acceleration, *Phys. Rev. Lett.* **101**, 145002 (2008).
- [32] Tzoufras, M. *et al.* Beam loading by electrons in nonlinear plasma wakes. *Phys. Plasmas* **16**, 056705 (2009).
- [33] Lotov, K. V. Fine wakefield structure in the blowout regime of plasma wakefield accelerators. *Phys. Rev. ST Accel. Beams* **6**, 061301 (2003).
- [34] Sosedkin, A. P. & Lotov, K. V. LCODE: a parallel quasistatic code for computationally heavy problems of plasma wakefield acceleration. *Nuclear Instr. Meth. A* **829**, 350-352 (2016).

Acknowledgements

This work was supported by the President's Doctoral Scholarship Award of University of

Manchester, the Cockcroft Institute core grant and STFC. The contribution of K. V. L. and A. P. S. is supported by The Russian Science Foundation, Grant no. 14-12-00043. The authors greatly appreciate the computing time from the clusters at the University of Manchester.

Author contributions

Y. M. L. and G. X. X. contributed to all aspects of this work; K. V. L. and A. P. S. contributed to the code development and provided with significant technical support and useful discussions; K. H. and O. M. A. gave many useful comments and suggestions to this work.

Additional information

Competing financial interests: The authors declare no competing financial interests.